# Analysis of Magnetic Resonance Spectroscopic Signals with Data-based Autocorrelation Wavelets

A. Schuck Jr.*, C. Lemke**, A. Suvichakorn** and J-P. Antoine**

***Abstract*— A new class of wavelet functions called data-based autocorrelation wavelets is developed for analyzing Magnetic Resonance Spectroscopic (MRS) signals by means of the continuous wavelet transform (CWT), instead of the traditional wavelet like Morlet wavelet. These new wavelets are derived from the normalized autocorrelation function from metabolite data and then used for detecting the presence of a given metabolite in a signal with a presence of many different components and finally for quantifying some of its parameters.**

## I. Introduction

Magnetic Resonance Spectroscopy (MRS) is a technique based in the interaction between atomic nuclei of a sample submitted to a strong static magnetic field and bursts of radio-waves. This results in a signal composed of many frequency components typical from the active nuclei of that sample and the chemical environment around them. One characteristic is that the amplitude of the time-domain contributions of each nuclei or the area in the frequency domain is proportional to the amount of those nuclei in the sample under test, which is then related to the concentration of the substance in the sample [1]. However, the MRS signal acquired at short echo-time contains contributions not only from metabolites, but also from water and macromolecules and lipids, with noise and distortion. Many techniques have been proposed in the literature to quantify the metabolite contributions. These techniques are based on time domain quantification or frequency domain quantification methods. A review on this subject can be found in [2] and [3]. In this paper, we apply the wavelet analysis to the MRS signals, with the aim of detecting the presence of specific metabolites in an arbitrary superposition. Analyzing in the time and scale domains simultaneously can provide more useful information than the Fourier transform which gives only spectral information. In addition, a small perturbation of a signal which may occur during the data acquisition will result only in a small, local modification of the wavelet transform. Among several types of wavelet transforms, the continuous wavelet transform (CWT) technique can estimate the frequency and amplitude of the spectral line directly from the phase and modulus of the wavelet transform. A review of this approach may be found in [4]. However, the formalism developed in that paper used exclusively the Morlet wavelet transform to analyze the MRS signals. Now, the efficiency of the CWT analysis can be improved if one uses an *a priori* knowledge about the signal. The idea presented here is to define wavelet functions directly from the MRS data themselves by the autocorrelation function of the MRS data signals, properly averaged to zero. We will proceed in two stages. In a first step, we start from a model FID signal, for instance a truncated Lorentzian (i.e. put to zero for times $t < 0$) and evaluate its performance. Then, in a second step, we start from real metabolite data. Here we face the additional problem that data are by the nature of the acquisition discrete, and thus also their autocorrelation function. Therefore an extra step based on interpolation/decimation is needed for using such discrete wavelets for a *continuous* wavelet transform. The outcome is that these wavelets look promising for the analysis of MRS signals. In particular, they are able to detect without ambiguity the presence of a given metabolite in a superposition of several metabolites and lipids.

*Electrical Eng. Dept. (DELET), Federal University of Rio Grande do Sul (UFRGS), Porto Alegre, RS, Brazil adalberto.schuck@uclouvain.be; schuck@ufrgs.br

**Institut de Recherche en Mathématique et Physique, Université Catholique de Louvain, B-1348 Louvain-la-Neuve, Belgium jean-pierre.antoine@uclouvain.be

## II. The autocorrelation wavelets

Let us start from the autocorrelation function of a given model signal and use it as adapted wavelet after proper normalization. The autocorrelation function estimator $R_{xx}(t)$ of an ergodic process time series $x(\tau)$ is defined by

$$R_{xx}(t) = \int_{-\infty}^{\infty} x(\tau)\overline{x(\tau - t)}\,\mathrm{d}\tau, \tag{1}$$

where the overline denotes the complex conjugate [5].

Now, be a signal $x_1(t)$ a one component Lorentzian spectral line as

$$x_1(t) = A_1 e^{-D_1 t} e^{i\omega_1 t}\,\theta(t),\ D > 0, \tag{2}$$

where $\theta(t)$ is the Heaviside function (or step function). This model allows us to find an autocorrelation function, whereas the "pure" Lorentzian spectral line cannot have an analytical autocorrelation function. Also this model looks more like a FID signals obtained *in vitro* than a pure Lorentzian one.

Thus, computing the autocorrelation function of $x_1$ by (1), we obtain the adapted wavelet

$$\psi_1(t) = \frac{A_1}{2D_1} e^{-D_1|t| + i\omega_1 t},\ -\infty < t < \infty, \tag{3}$$

with Fourier transform

$$\Psi_1(\omega) = \frac{A_1^2}{D_1^2 + (\omega - \omega_1)^2}. \tag{4}$$

The function obtained is localized and oscillating, but to make this wavelet function admissible, it is necessary to

introduce an additive correction term, as for the Morlet wavelet [10]. But here too, the correction term is numerically negligible for realistic values of the parameters, so we will omit it.

The CWT of the signal $x_1(t)$ with the wavelet $\psi(t)$, evaluated in the frequency domain, is:

$$S_1(b,a) = \frac{1}{2\pi}\sqrt{a}\int_{-\infty}^{\infty} \overline{\Psi_1(a\omega)}\, X_1(\omega)\, e^{i\omega b}\, \mathrm{d}\omega \tag{5}$$

$$= \sqrt{a}\, x_1(b) \frac{A_1^2}{D_1^2 + [\omega_1(a-1) + iaD_1]^2}\,, \tag{6}$$

where $\overline{\Psi_1(\omega)}$ means the complex conjugate of the Fourier transform of $\psi_1(t)$, $a > 0$ and $b \in \mathbb{R}$ are the scaling and translation variables, respectively.

It can be seen that the CWT diverges as $a \to 1$ (the match between the wavelet and the signal is too perfect!). But choosing different damping factors for the signal and the wavelet, namely $D_{11}$ and $D_1$, respectively, we get for $a = 1$:

$$|S_1(b,1)| = e^{-D_{11}b}\, \frac{|A_1^2|}{|D_1^2 - D_{11}^2|}\,. \tag{7}$$

and one can estimate the damping factor of the signal by:

$$D_{11} = -\frac{d}{db} \ln |S_1(b,1)|\,. \tag{8}$$

This behavior changes, if we have more than one component, i.e. a sum of Lorentzian lineshapes. For a left truncated signal $x_2(t)$ with two components as

$$x_2(t) = \left[A_1 e^{-D_1 t} e^{i(\omega_1 t + \phi_1)} + A_2 e^{-D_2 t} e^{i(\omega_2 t + \phi_2)}\right] \theta(t)\,, \tag{9}$$

its Fourier transform is

$$X_2(\omega) = \frac{A_1}{[D_1 + i(\omega - \omega_1)]} + \frac{A_2}{[D_2 + i(\omega - \omega_2)]}\,, \tag{10}$$

and the autocorrelation wavelet derived from (10) is given by

$$\Psi_2(\omega) = \frac{A_1^2}{[D_1^2 + (\omega - \omega_1)^2]} + \frac{A_2^2}{[D_2 + (\omega - \omega_2)^2]} + \frac{2[D_1 D_2 + (\omega - \omega_1)(\omega - \omega_2)]}{[D_1^2 + (\omega - \omega_1)^2][D_2 + (\omega - \omega_2)^2]}\,. \tag{11}$$

If the peaks are sharp enough and far away from each other, the third term in (11) will be numerically negligible and can be omitted. Then, the CWT of the signal $x_2(t)$ using this wavelet becomes

$$S_2(b,a) = \sqrt{a}\left\{\sum_{k=1}^{2} \frac{A_k^2 x_k(b)}{D_k^2 + [a(\omega_k + iD_k) - \omega_k]^2} + \frac{A_1^2 x_2(b)}{D_1^2 + [a(\omega_2 + iD_2) - \omega_1]^2} + \frac{A_2^2 x_1(b)}{D_2^2 + [a(\omega_1 + iD_1) - \omega_2]^2}\right\}. \tag{12}$$

The terms in the sum are similar to (6), giving a local maximum at $a = 1$ and interacting with each other so that one cannot use them for estimating the damping factors. On the other hand, the last two terms will give local maxima at scales $a = \omega_j/\omega_k$, $j \neq k$. In this case, assuming again that the peaks are sharp and far enough from each other and that the damping factors of the signal (namely $D_{11}$ and $D_{22}$) are different from those of the wavelet, then the latter can be estimated by $D_{11} \approx -\frac{d}{db}\ln|S_2(b, \frac{\omega_2}{\omega_1})|$ and $D_{22} \approx -\frac{d}{db}\ln|S_2(b, \frac{\omega_1}{\omega_2})|$. Figs. 1a and 1b show $|S_L(b,a)|$ for a one peak ($L = 1$) and and a two peak-signals ($L = 2$) and wavelets for $A_1 = A_2 = 1$, $D_1 = D_2 = 1$, $\omega_1 = 32$ and $\omega_2 = 64$ rad/s. This method can be further generalized for multipeak signals but we will refrain from doing it here.

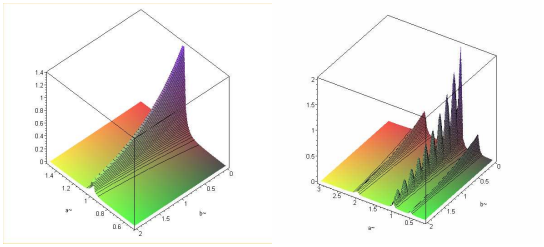

(a) (b)

Fig. 1. $|S_L(b,a)|$ for (a) One peak and, (b) Two-peak signals and wavelet for $A_1 = A_2 = 1$, $D_1 = D_2 = 1$, $\omega_1 = 32$ and $\omega_2 = 64$ rad/s, $b = [0,2]$ and $a = [0.5, 1.5]$ and $a = [0.2, 3]$ in the two-peak case.

## III. Metabolite-based wavelets

Now we turn to more realistic signals and apply the method developed above to signals limited in time, that is, vanishing outside some interval $[0, T_0]$, for some finite $T_0$. First, we analyze numerically a discretized $L$-component signal $x_L[n]$, defined as

$$x_L[n] = \begin{cases} 0, & 0 \leqslant n \leqslant \frac{N}{4} - 1, \\ \sum_{l=1}^{L} A_l\, \psi_l[n], & \frac{N}{4} \leqslant n \leqslant \frac{3N}{4} - 1, \\ 0, & \frac{3N}{4} \leqslant n \leqslant N - 1, \end{cases}$$

where $N$ is the length of the signal in samples, each $\psi_l[n] = e^{-D_l[n - \frac{N}{4}]t_s}\, e^{i\omega_{sl}[n - \frac{N}{4}]t_s}$ is a single Lorentzian component, $L$ is the number of components and $t_s$ is the sampling period in seconds. We perform the CWT analysis for the $L = 1$ and the $L = 2$ signal with $N = 4096$ samples using the YAWTB toolbox [6].

The results are shown in Figures 2a to 2d.

Both results exhibit strong horizontal ridges (lines of local maxima) for $a = 1$ and this indicates that the component $x_1$ or $x_2$ are present in the signal. This feature will be the crucial ingredient for detecting a given signal (pure metabolite) in an unknown superposition. Also, for the two-peak signal and wavelet, one notices the presence of two horizontal ridges at $a = 0.5$ and $a = 2$, which correspond to the ratios between frequencies of the signal and the wavelet. The estimation of damping factors was made for the scales 0.5 and 2 of $|CWT\{x_2[n]\}|$ for $A_1 = A_2 = 1$, $D_{11} = 0.9$ and $D_{22} = 1.1$, $\omega_1 = 32$ and $\omega_2 = 64$ rad/s, $t_s = 1/256$ s. Here zeros were added to extremities of signal to reduce estimation artifacts, before the CWT be performed. The result is shown in Fig. 3. In the central part of the figure ($5000 \leq n \leq 6000$), one

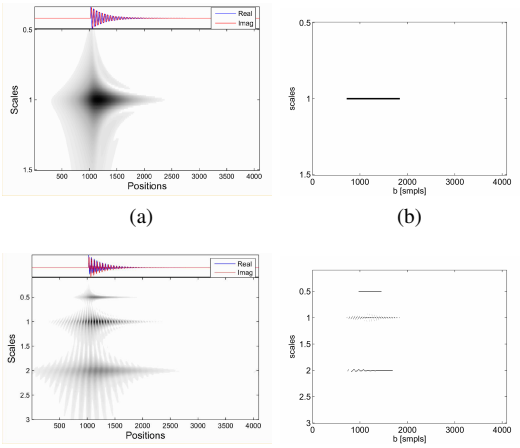


(a) (b)

(c) (d)

Fig. 2. (a) $|CWT\{x_1[n]\}|$ and (b) horizontal ridges of $|CWT\{x_1[n]\}|$, (c) $|CWT\{x_2[n]\}|$ and (d) horizontal ridges of $|CWT\{x_2[n]\}|$ for $A_1 = A_2 = 1$, $D_1 = D_2 = 1$, $\omega_1 = 32$ and $\omega_2 = 64$ rad/s, $t_s = 1/256$ s and $N = 4096$.

does obtain the correct values of the damping factors, but for multipeak signals, this estimation proves to be a hard task and more effort should be made on that.

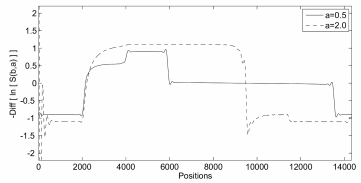


Fig. 3. Estimation of damping factors made at the scales $a = 0.5$(line) and $a = 2$ (dash) of $|CWT\{x_2[n]\}|$ for $A_1 = A_2 = 1$, $D_{11} = 0.8$ and $D_{22} = 1.2$, $\omega_1 = 32$ and $\omega_2 = 64$ rad/s, $t_s = 1/256$ s.

Next, we derive our metabolite-based wavelets from metabolite profiles, acquired by MRS measurements of phantoms filled with single metabolites or by simulation in jMRUI [7]. Here, these profiles have been simulated quantum mechanically at ESAT, K.U.Leuven, with NMRSCOPE [8] using a PRESS sequence, an echo time of 30 ms, and a field strength of 1.5T. Among these, we will exploit two particular cases, Creatine (Cre) and Lactate (Lac). Each of those wavelets is supposed to be sensitive to one metabolite and were calculated by the discrete form of $R_{xx}(t)$ for each profile $\phi_m(n)$, named $R_m[n]$ and given by

$$R_m[n] = \sum_{k\in\mathbb{Z}} \phi_m[k]\,\overline{\phi_m[k-n]},\ m = 1,\ldots,K, \qquad (13)$$

where the overline denotes the complex conjugate, $K$ is the number of metabolite profiles and $m$ indexes the profiles. As the metabolite profile $\phi_m$ in MRS is a mixture of decaying, complex oscillations, its autocorrelation values are complex, too. Since the signal is limited, we removed its mean value numerically in order to make an admissible wavelet from this function so that

$$\psi_m[n] = R_m[n] - \mathrm{E}\{R_m[n]\};\ m = 1,\ldots,K, \qquad (14)$$

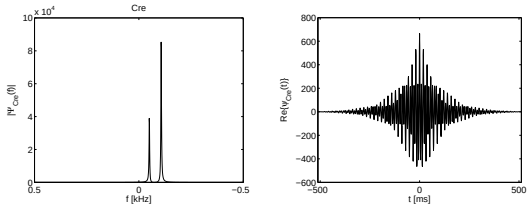


(a) (b)

Fig. 4. Wavelet constructed from simulated Creatine (Cre) profile: (a) Modulus of the Cre-based wavelet spectrum; (b) Real part of the Cre-based wavelet in time domain.

where $K$ is the number of metabolite profiles and $m$ indexes the wavelet function to the profiles.

To give an example, we take a simulated Creatine (Cre) profile. Fig. 4a) shows the absolute value of the corresponding Cre-based wavelet, in frequency domain. It shows two characteristic peaks as the original Creatine profile in the frequency domain. Fig 4b shows the real part of this wavelet in time domain. One can see that the function obtained is well localized and has zero mean, as required for an admissible wavelet. The same operation was performed for all the metabolites and lipids contained in the data base.

Since these wavelets are numerical and discrete, performing the CWT requires to dilate them. To do that it was used an upsampler/downsampler system as proposed in [9] it is used because changing the scale corresponds to choosing another sampling frequency in the discrete case. First expand the signal by an integer factor of $L$ by inserting $L-1$ zeros between the original samples and then calculate these values with a low-pass digital filter with cutoff frequency of $\pi/L$ rad (here a Bartlett window of length $2L-1$). After the signal is again low-pass filtered in order to avoid aliasing effects by a filter with cutoff frequency of $\pi/M$ rad (here a 128 tap FIR filter in MATLAB©). With this procedure, our possible scales will be $a = L/M$. To perform a CWT analysis, the set of dilated wavelets are created at the desired scales, aligned and their length made equal by zero padding at the extremities. Then, their FFT are taken as the signal. The CWT is obtained by multipling the spectra of the signal by the wavelet spectra and then taking the IFFT of the result (this is the discrete version of (5)).

In order to estimate the efficiency of the method, two noise-free signals were created: (a) one composed of a sum of all metabolites and lipids available from the data base, shown in Fig. 5a ;(b) the second, exactly the same signal, but with the Lactate component removed, shown in Fig. 5b. The difference between the two spectra can hardly be seen.

Next we apply the CWT with the metabolite-based wavelets to the two composed signals of Figure 5, in order to see if the metabolites could be detected. The upper panel of each figure shows the modulus of CWT coefficients in a time-scale representation. The lower panel shows the horizontal ridges as an indicator of local maxima along the time axis.

First, we show the analysis with the Cre-based wavelet.

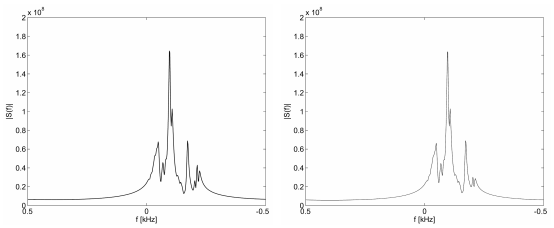


(a) (b)

Fig. 5. Example of a composed MRS signal: (a) including all metabolites from the data base; (b) the same as (a), but with the Lac contribution removed.

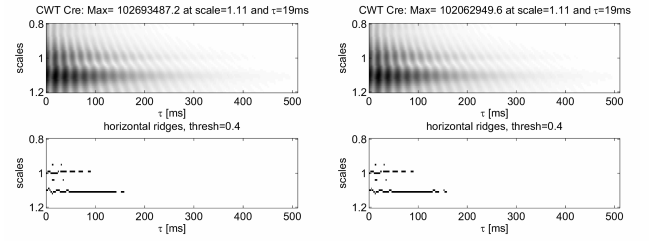


(a) (b)

Fig. 6. CWT using the Cre-wavelet on (a) The composed signal from Fig. 5a; and (b) The same without Lac. The presence of Cre is indicated by the local maxima at scale $a = 1$.

When applied on the composed signal with Lac, the outcome is not a straight line (Fig. 6a). However, it still shows significant local maxima at scale $a = 1$, which are characteristic for the presence of this metabolite. The same result is obtained on the composed signal without Lac, there are only some minor differences in the amplitudes of the maximum CWT magnitude (Fig. 6b).

Then we turn to the Lac-wavelet. The CWT with the Lac-based wavelet of the composed signal exhibits a significant structure at the scale $a = 1$ (Fig. 7a). Again, this indicates the presence of Lac in the composed signal. But when we analyze the composed signal without Lac, that structure at scale $a = 1$ disappears as it should (Fig. 7b).

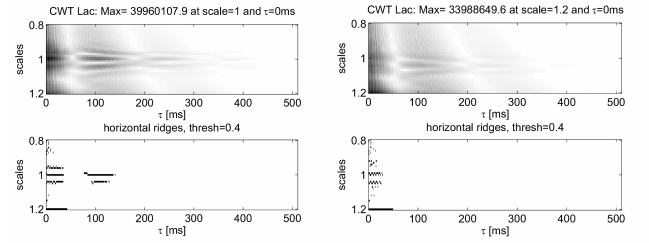


(a) (b)

Fig. 7. CWT using the Lac-wavelet on (a) The composed signal from Fig. 5a and (b) The same without Lac. The presence of Lac is indicated by the local maxima at scale $a = 1$ in (a) but not in (b), since Lac is no longer included.

## IV. Conclusion

The conclusion of the preceding analysis is that these metabolite-based wavelets are able to identify without ambiguity the presence of the corresponding metabolite in a composed signal, simply by viewing local maxima in the wavelet transform. The method works also in the presence of noise, which makes it more realistic for application to *in vivo* signals. In addition, using an approximate expression for the wavelet spectrum of a composed signal, these wavelets allow us also to estimate the amplitude of each metabolite contained in the mixture. This aspect, however, requires further work, as well as designing a fully automated algorithm based on the present technique.

## Acknowledgment

This work is part of the Advanced Signal Processing for Ultra-fast Magnetic Resonance (FAST) project funded by the Marie-Curie Research Network (MRTN-CT-2006-035801) `http://fast-mrs.eu`.

A. Schuck Jr. thanks the Conselho Nacional de Pesquisa e Desenvolvimento - CNPq, Brazil, for its financial support.

C. Lemke and A. Suvichakorn were ER Marie-Curie Fellows until January and June, 2010, respectively.

The authors would also like to express their gratitude to Prof. S. van Huffel (K.U. Leuven) and Prof. D. van Ormondt (TU Delft) for their invaluable advice.

## References

[1] J.P.Hornak. *The Basics of NMR*. Department of Chemistry, Rochester Institute of Technology, Rochester, NY, 1997. http://www.cis.rit.edu/htbooks/nmr/.

[2] L. Vanhamme, T. Sundin, P. Van Hecke, and S. Van Huffel. MR spectroscopic quantitation: A review of time domain methods. *NMR Biomed.*, 14(4): 233–246, 2001.

[3] S. Mierisova and M. Ala-Korpela. MR spectroscopy quantitation: a review of frequency domain methods. *NMR Biomed.*, 14(4): 247–259, 2001.

[4] A. Suvichakorn, H. Ratiney, A. Bucur, S. Cavassila, and J-P. Antoine, Toward a quantitative analysis of *in vivo* magnetic resonance proton spectroscopic signals using the continuous Morlet wavelet transform, *Meas. Sci. Technol.* 20, paper #104029 (11 pages), 2009.

[5] A. Papoulis and S.U. Pillai, *Probability, Random Variables and Stochastic Processes*. McGraw-Hill, NY, 4th edition, 2002.

[6] L. Jacques, A. Coron, P. Vandergheynst, and A. Rivoldini, The YAWTb toolbox : Yet Another Wavelet Toolbox, 2007. http://rhea.tele.ucl.ac.be/yawtb.

[7] See `http://sermn02.uab.cat/mrui/mrui_Overview.shtml`

[8] D. Graveron-Demilly, A. Diop, A. Briguet, and B. Fenet, Product-operator algebra for strongly coupled spin systems, *J. Magn. Reson. A*, 101(3): 233239, 1993.

[9] A. Oppenheim, R.W. Schaffer, and J.R. Buck *Discrete-Time Signal Processing*. Prentice-Hall, Englewood Cliffs, NJ, 2nd edition, 1999.

[10] B. Torrésani *Analyse continue par ondelettes*. InterEditions & CNRS Editions, Paris, 1995.